Energy-Absorbing Capacity of Cellular Textile Composites: Modeling and Optimization

T.X. Yu[1], P. Xue[1] and X.M. Tao[2]

[1]Department of Mechanical Engineering, Hong Kong University of Science and Technology, Clear Water Bay, Kowloon, Hong Kong
[2]Institute of Textile and Clothing, Hong Kong Polytechnic University, Hung Hom, Kowloon, Hong Kong

SUMMARY: In our previous studies a new type of cellular textile composites was developed and it demonstrated high specific energy-absorbing capacity. In the cellular structure, each cell contained a hemispherical shell connected to a truncated conical wall (Configuration 1). A theoretical model is proposed to quantify the contributions to energy dissipation from different deformation stages. Theoretical and experimental results show that large plastic deformation of the truncated conical shell contributes most to the total energy absorption. Therefore, a new cell configuration is proposed, in which each cell is a truncated conical shell only (Configuration 2). In comparison with Configuration 1, the grid-domed textile composite with Configuration 2 displays a higher energy-absorbing capacity, lower peak force and almost constant force magnitude during its large deformation process. The effects of the cell height, the diameter ratio of cell-top to cell-bottom and the resin added-on percentage on the energy-absorbing capacity are also investigated.

KEYWORDS: energy, absorption, textile, cellular.

1. INTRODUCTION

Energy absorption characteristics is one of the most important topics in selecting materials for many engineering applications, such as crushing elements in cars, bicycle's helmets, hard hats used in construction sites and protective packaging of fragile goods, etc. As summarized by Johnson & Reid [1] and Yu [2], the materials or devices used as impact energy absorbers should utilize the inelastic deformation as its major energy-absorbing mechanism, the force required for its deformation should remain almost constant, and the deformation stroke should be long and in a stable mode. In addition to these requirements, attributes of lightweight can also play an important role in the applications listed above.

Cellular solids, which contain a large amount of space and normally have a relative low density, possess excellent energy absorption capacity. Previous studies on the behaviour of cellular materials have been mainly limited to polymer foams [3,4], honeycombs (under lateral load [5,6] or axial load [7]), metal ring systems and tube arrays [8,9,10] and woods [11,12]. Only in last few years, the energy-absorbing capacity of textile composites has attracted attention of researchers. The energy-absorption behaviour of textile composites have been investigated through several components, such as the braided composite I-beams for crushing elements in cars [13], triaxially braided composite square tubes as crushing elements [14,15] and 3-D woven sandwich structure [16].

In our previous studies we investigated a range of grid-domed cellular textile composites in term of their energy-absorption behaviour under quasi-static compression and impact condition [17-19]. The present paper will present a theoretical model to study the quasi-static and dynamic behaviour of grid-domed textile composites, based on which this kind of cellular textile composite can be optimized in view of its specific energy-absorbing capacity.

2. MATERIALS AND SAMPLES WITH CONFIGURATION 1

The reinforcements for the grid-domed composites were knitted fabrics made of multi-filament textured nylon yarns. In order to characterize the quasi-static mechanical properties of the double jersey-nylon (DJ-N) type, flat composite samples with similar percentage of polymer add-on, which had been rigidized by the same process as grid-domed cellular composites, were tested under tension and bending conditions [19]. For the simple tension samples with size 200mm×20mm×1mm, the loading-unloading curves are shown in Fig. 1, which demonstrate significant visco-elasticity. The flat fabrics were formed into a 3D cellular structure by a two-step method, forming and consolidation by a polyester resin. The cells were arranged in a grid pattern, whilst each cell contained a hemispherical cap connected to a truncated conical wall (Configuration 1). The schematic geometry of this configuration is shown in Fig. 2.

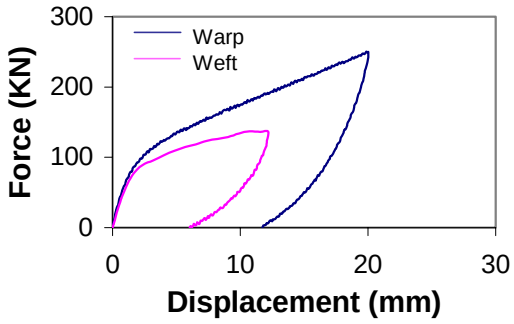

Fig. 1: Loading-unloading;

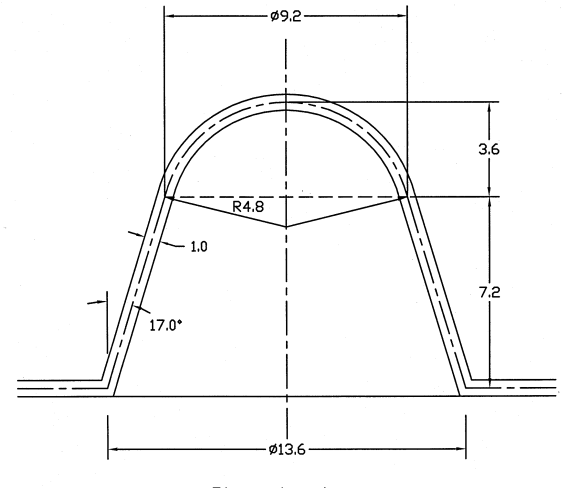

Fig. 2: Schematic geometry of a cell of samples with Configuration 1.

3. MECHNICS MODELS OF GRID-DOMED TEXTILE COMPOSITES

As observed in both quasi-static and impact tests, the major deformation mechanism for grid-domed composite samples DJ-N is the collapse of the shells, including both hemispherical cap and truncated conical wall in the cell (a single cell is shown in Fig. 3). In the following, three

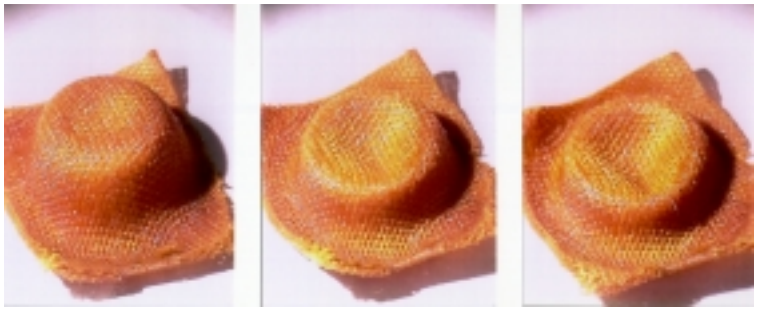

Fig. 3: Deformation process of a grid-domed composite sample DJ-N.

successive theoretical models are proposed for the observed three stages of the deformation process, respectively, so as to predict the force-displacement relationship and the energy-absorbing capacity.

3.1 Stage 1: Local inversion of a hemispherical dome

As well known, when a hemispherical dome is subjected to a concentrated force at its apex or compressed by a rigid flat plate on its top, elastic or elastoplastic snap-through will occur, depending on the dimension of the dome and the material's properties. Apart from numerous elastic analyses, based on an analysis given by Updike [20], a simple but profound rigid-plastic model was presented by Calladine [21, 22]. Figure 4 shows, schematically, the local inversion model employed by Updike and Calladine, under a compression of a rigid flat plate subjected to an inward-directed force *P*. At any instant in the process, the inverted region is separated from the outer portion of the hemispherical dome by a narrow toroidal "knuckle", that moves outwards as deformation proceeds. The knuckle region is connected to the two spherical portions by two travelling circumferential plastic hinge circles, of radius e ± *l*/2, with *l* being the meridian extent of the knuckle.

By formulating and solving the equations which have been obtained by proper consideration of the kinematics, equilibrium and constitutive relations of the problem, it is finally obtained that [20-22]

$$l = \sqrt{3/2}R^{0.5}h^{0.5} = 1.22R^{0.5}h^{0.5} \tag{1}$$

$$P_1 = 2\pi\sqrt{3}Yh^{1.5}w^{0.5} = 10.9Yh^{1.5}w^{0.5} = 43.6M_o(w/h)^{0.5} \tag{2}$$

where Y is the uniaxial yield stress of the material, $M_o = Yh^2/4$ is the fully plastic bending moment per unit width of the shell, and w is the vertical displacement of the rigid plate applied on the top of the hemispherical dome. Subscript 1 of the applied force pertains to deformation Stage 1.

If each grid-domed sample contains n domes, the total force applied on the sample will be

$$(P_1)_{\text{total}} = n \times P_1 = 43.6\, nM_o(w/h)^{0.5} \tag{3}$$

Accordingly, the energy dissipation from $w = 0$ to a certain displacement w can be calculated as

$$W_1 = \int_0^w (P_1)_{total}\, dw = 29.1nM_o w^{1.5}h^{-0.5} \tag{4}$$

Equations (3) and (4) provide a theoretical force-displacement relationship and an estimate of the energy-absorbing capacity, respectively, of the grid-domed cellular textile composites in their early stage (i.e. Stage 1) under compression or impact loading.

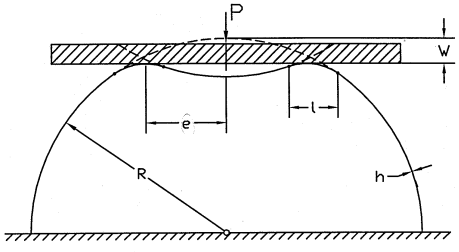

Fig. 4: Schematic diagram of local inversion model.

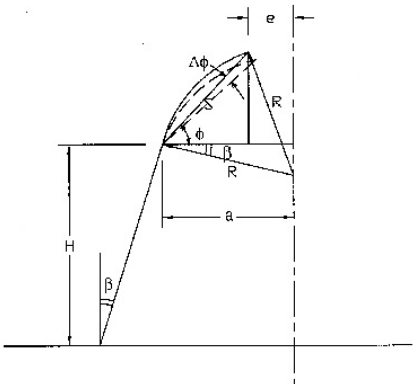

Fig. 5: Deformed configuration in stage 2.

3.2 Stage 2: Global plastic collapse of a truncated spherical cap

The above local inversion mechanism of the hemispherical domes is applicable only when the support of the spherical dome at its base circle remains fixed, so this mechanism will cease to be valid when the applied force is so large that a plastic hinge circle forms at the base of the partial spherical cap followed by a multi-hinge deformation mechanism occurred in the truncated conical shell underneath the spherical cap, see Stage 3 described below.

Since the spherical dome has been deformed in Stage 1, the analysis of Stage 2 is based on the deformed configuration (Fig. 5). By assuming that a plastic hinge circle forms at the base of the truncated spherical cap and assessing the plastic energy dissipation by both bending and membrane deformations, a force-displacement relationship can be established as

$$\frac{P_2}{M_o} = \frac{\pi \times \cos\beta}{\cos\phi \cos(\phi+\beta)} + \frac{16\pi R}{3h} \times \tan\phi \sin\phi \cos(\phi+\beta) \tag{5}$$

and (refer to Fig. 5)

$$w = R \times [1 - \sin\beta - 2\cos(\phi+\beta)\sin\phi] \tag{6}$$

where angle β is specified by the original spherical cap, and angle ϕ, which can be calculated from *w/R* by using Eqn (6), will serve as a process parameter.

When the force required by the global plastic collapse mechanism of the truncated spherical cap calculated by Eqn. 5, P_2, is greater than the force required by the local inversion of the spherical cap calculated by Eqn. (2), P_1, the local inversion will continue to develop. However, when $P_2 < P_1$, the global collapse mechanism will take over and the local inversion ceases to develop.

3.3 Stage 3: Large plastic deformation of a truncated conical shell

After a plastic hinge forms at the connecting circle between the spherical cap and the truncated conical shell, bending moments as large as the fully plastic bending moment begin to apply on the top of the truncated conical shell. When the partial spherical shell rotates about the plastic hinge circle at its base, this bending moment and the compression force produced by the rigid flat plate applied on the top of the dome will initiate a multi-hinge deformation mechanism in the truncated conical shell (shown in Fig. 6). At this deformation stage (i.e. Stage 3), although the bending along the hinge lines and the bending of the conical shell in the circumferential direction will make a certain contribution to the energy dissipation, the energy-absorbing capacity of the cell is dominated by the membrane deformation of the conical shell, especially when the total vertical displacement becomes very large.

In the membrane-dominated deformation mechanism, merely the energy dissipated by the compression of the generators of the truncated conical shell is accounted. By noting that DJ-N samples display a bi-linear stress-strain relation in their tensile behaviour (refer to Fig. 1), this analysis concludes that, in Stage 3, a linear relation, as given by equation (7), can be established between the compression force and the vertical displacement; whilst the slope of the force-displacement curve can be predicted accordingly by the following simple expression:

$$(P_3)_{total} = 2\pi nRh\cos\beta \times (Y + \Delta w \times E_p \cos\beta / 4H) \tag{7}$$

$$\frac{d(P_3)_{total}}{d(\Delta w)} = \pi n \frac{Rh}{2H} E_p \cos^2\beta \tag{8}$$

which represents a linear relation between the force required and the increment of the vertical displacement from the top, Δw.

3.4. Estimation of the energy-absorbing capacity of grid-domed composite samples

Based on our experimental data, Stage 3 contributes most to the total energy-absorption of DJ-N samples. It may be suggested, therefore, to employ Eqn (8) to estimate of the total energy-absorbing capacity W_w of these composites till any displacement w, before densification happens. Thus, integrating Eqn (8) twice leads to

$$W_w = \int_0^w (P_3)_{total}\, dw \cong n\frac{\pi Rh}{4H} E_p \cos^2\beta \times w^2 \tag{9}$$

Accordingly, when the energy absorption per unit mass of the sample is concerned, the following simple expression can serve as an estimate:

$$\frac{W_w}{m} = \frac{\pi Rh}{4\mu H} E_p \cos^2\beta \times w^2 \tag{10}$$

where W_w denotes the energy absorption of the sample until displacement w, m denotes the mass of the sample and μ denotes the mass of a unit cell. In a more general case, E_p can be regarded as the average tangential modulus of the material during its plastic deformation.

Eqn. (10) is valid for the grid-domed textile composites of Configuration 1 studied under quasi-static compression. To estimate the energy-absorbing capacity of these cellular composites under impact or compression at a high rate, Eqn (10) can be combined with strain-rate effect of this material, leading to

$$\frac{W_w}{m} = \left\{\frac{\pi Rh}{4\mu H} E_p \cos^2\beta \times w^2\right\} \times \left\{1 + \frac{B}{A}\log\left(\frac{\dot{c}}{\dot{c}_o}\right)\right\} \tag{11}$$

where A and B are the experimentally determined constants and $\dot{c}_o$ is a low compression-rate served as the basis of comparison.

The prediction of the above deformation models was found to be in excellent agreement with our experimental results [19].

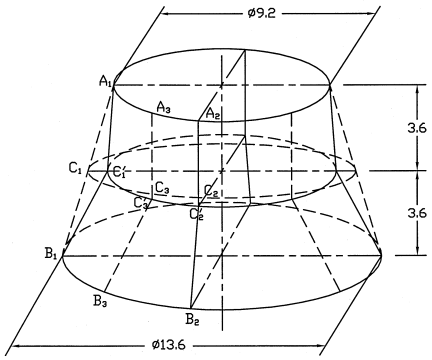

Fig. 6: Multi-hinge deformation mechanism in Stage 3.

Fig. 7: A sample with Configuration 2.

4. OPTIMIZING ENERGY-ABSORBING CAPACITY OF GRID-DOMED TEXTILE COMPOSITES

As illustrated above, the deformation process of a cell with Configuration 1 consists of three stages, but Stages 1 and 2 are much shorter and make much less contribution to the total energy absorbed. In other wards, the energy absorption is mainly attributed to the plastic deformation of the truncated conical shells.

Accordingly, a new cell configuration has been designed (Configuration 2), in which each cell consists of a truncated conical shell only, as shown in Fig. 7. The materials used here were the

same as those for Configuration 1. Impact tests were conducted under impact velocities of 3.4-4.8 m/s. Under the identical test condition for samples with 100×100 mm^2 and the same weight, the load-time curves and energy-displacement curves for the two configurations are given in Fig. 8 and Fig. 9, respectively. The energy-absorbing capacities for both configurations are summarized in Table 1, where the data in the columns with unit J denote the total energy dissipated, and those with unit J/g denote the energy dissipation per unit weight of the sample.

The data in Table 1 indicate that, compared with those of Configuration 1, the grid-domed textile composites of Configuration 2 have a higher energy-absorbing capacity (i.e. 2.7-3.3 time up to 4mm vertical displacement, and 1.4-1.8 time up to 8mm vertical displacement), low peak force and almost constant magnitude of force during their large deformation process.

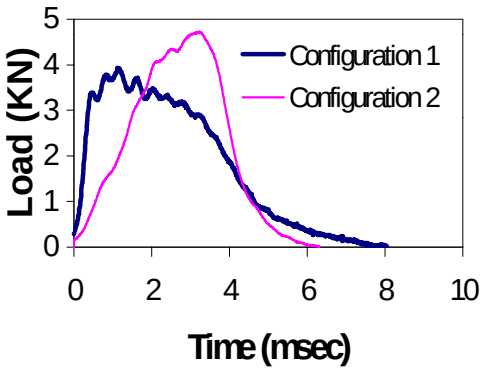

Fig. 8: Load-time curves for samples of two configurations.

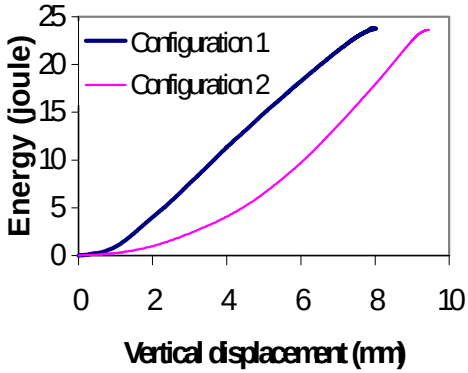

Fig. 9: Energy-displacement curves for samples of two configurations.

Table 1. Comparison of energy-absorbing capacity for both configurations

E_0 : impact energy V_0 : impact velocity		Energy absorption Up to 4 mm Displacement		Energy absorption Up to 8mm Displacement	
		J	J/g	J	J/g
E_0 =23 J V_0 =3.47 m/s	Conf. 1	3.42	0.45	16.11	2.15
	Conf. 2 H=13.8mm	11.39	1.08	23.74	2.26
E_0 =45±2% J V_0 =4.8 m/s	Conf. 1	4.10	0.54	16.46	2.19
	Conf. 2 H=13.8mm	11.02	0.96	28.0	2.43

5. INFLUENCE OF CELL GEOMETRY AND RESIN ADD-ON UPON ENERGY-ABSORBING CAPACITY

In order to further optimize the characteristics and energy-absorbing capacity of the grid-domed textile composites, cell height and diameter ratio of cell top to cell bottom were selected to explore the influence of geometry on the mechanical properties and energy-absorbing capacity. The effect of resin added-on percentage on the energy-absorbing capacity was also investigated.

Figures 10 and 11 depict the curves of load vs. vertical displacement and the energy dissipation per unit weight vs. vertical displacement under the impact velocity of 3.54 m/s and impact energy of 26 joule for the samples with the same level of resin added-on and same diameter ratio of cell-top to cell-bottom, but different cell heights. Cell heights in the range

from 7.84 mm to 15.72 mm were examined, while the corresponding semi-apical angles of the truncated conical shell varied from 27° to 14°. The peak force of curve 1 was resulted from the contact between the tup and the supporting base. Hence, the cell height should not be too

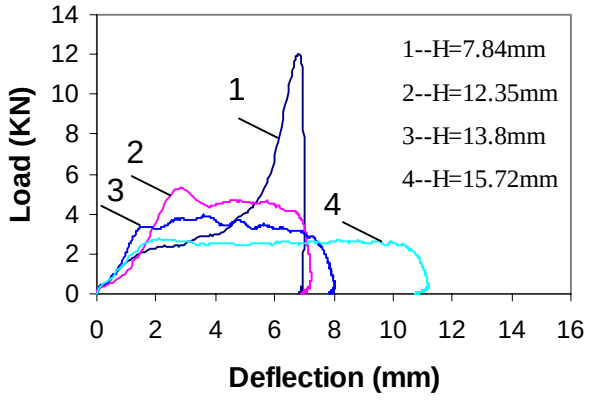

Fig. 10: Comparison for load vs. vertical displacement.

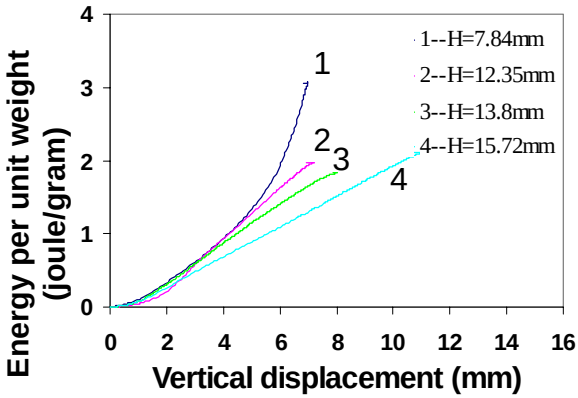

Fig. 11: Comparison for energy per unit weight vs. vertical displacement.

small for obtaining higher energy-absorbing capacity. From other three samples, it is evident that the magnitude of load reduced and the total stroke increased with the increase of the cell height. The samples with higher cells generally possess greater potential of energy absorption in a longer stroke, although their energy-absorbing capacity is restricted when the impact velocity is small.

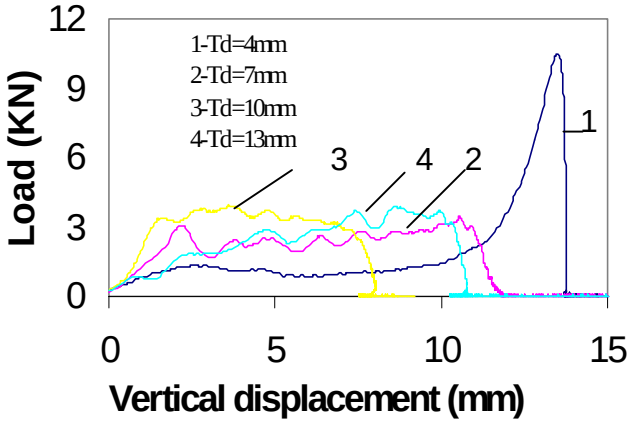

Fig. 12: Comparison for load vs. vertical displacement.

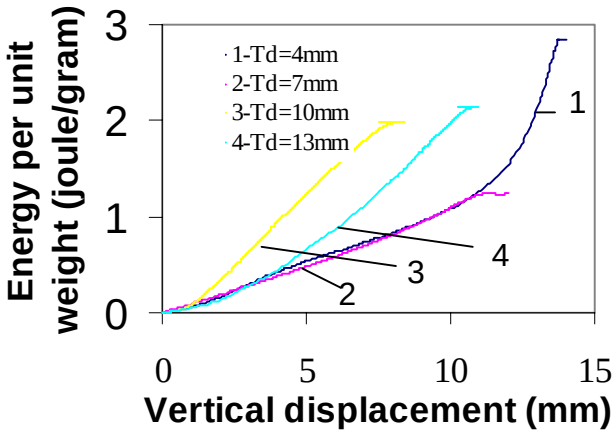

Fig. 13: Comparison for energy per unit weight vs. vertical displacement.

Figures 12 and 13 present the curves of load vs. vertical displacement and energy per unit weight vs. vertical displacement under the impact velocity of 3.50 m/s and impact energy of 25.9 joules for the samples with the same percentage of resin added-on and the same cell height, but different diameter ratio of cell-top to cell-bottom. The top diameter of a cell varied from 4 mm to 13 mm, whilst the bottom diameter remained constant. From the test results, it is evident that the smaller top diameter is not beneficial to energy-absorbing capacity of the composite. The optimal top diameter within the examined parameter range is 10 mm.

Figures 14 and 15 depict the curves of load vs. vertical displacement and energy per unit weight vs. vertical displacement under the impact velocity of 4.80 m/s and impact energy of 48.5 joules for the samples with the same cell dimensions, while the percentage of resin added-on varied from 155% to 240%. From the figures, it is found that the percentage of resin

added-on has little difference on the specific energy-absorbing capacity within the investigated range.

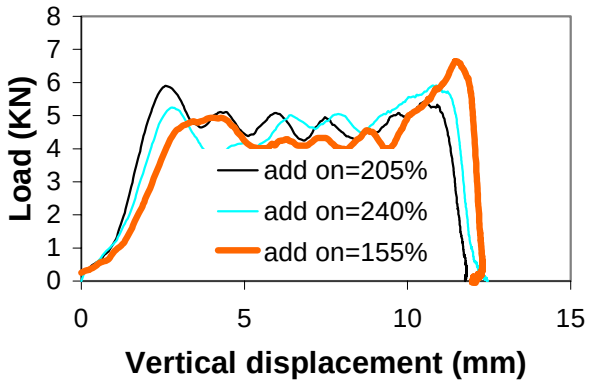

Fig. 14: Comparison for load vs. vertical displacement.

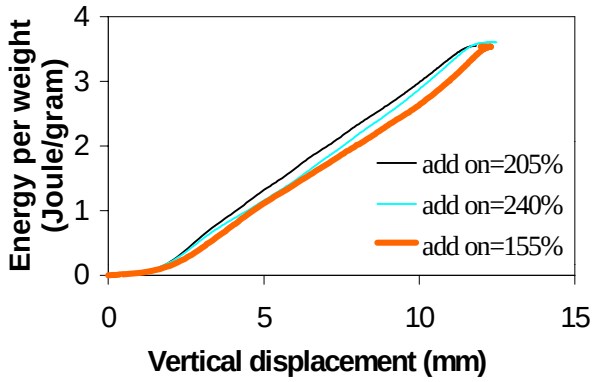

Fig. 15: Comparison for load vs. vertical displacement.

CONCLUSION

The energy absorbing capacity of the grid-domed textile composite can be predicted well by the theoretical models proposed in the paper, especially in Stage 3.

Compared with samples of Configuration 1, samples of Configuration 2 possess lower peak force, almost constant force magnitude during its large deformation process and considerably higher specific energy-absorbing capacity.

The higher the cell, the lower the peak load and the greater potential for energy absorption in a longer stroke. The energy-absorbing capacity also varies with the diameter ratio of cell-top to cell-bottom. Under the condition of constant cell height of 13.8 mm, the optimal top diameter is found to be 10 mm for the examined parameter range. The resin added-on exhibits little influence in the energy-absorbing capacity of grid-dome textile composites for the examined range.

ACKNOWLEDGMENT

The authors would like to thank the Hong Kong Research Grant Council (RGC) for the support to this research under contract HKUST 6017/98E.

REFERENCES

[1] Johnson W. and Reid S.R., "Metallic Energy Dissipating Systems", *Applied Mechanics Review, ASME*, 1977, pp. 277-288.
[2] Yu T.X, "Energy-Absorbing Devices Utilizing Plastic Deformation of Metals", *Advances in Mechanics*, Vol. 16, No. 1, 1986, pp. 28-39.
[3] Gibson, L.J. and Ashby, M.F., "*Cellular Solids: Structure and Properties*". Pergamon Press, New York, 1988.
[4] Mills, N.J., Chapter 9 in *Low Density Cellular Plastics, Physical Basis of Behaviour* (eds. N.C. Hilyard and A. Cunningham). Chapman and Hall, London, 1994.
[5] Klintworth, J.W. and Stronge, W.J., "Elasto-Pastic Yield Limits and Deformation Laws for Transversely Crushed Honeycombs", *Int. J. Mech. Sci.*, Vol. 30, 1988, pp. 273-292.

[6] Stronge, W.J., "Dynamic Crushing of Elastoplastic Cellular Solids", In *Mechanical Behaviour of Materials IV* (ICM6), Vol.1 (M. Jono and T. Inoue Eds.). Pergamon Press, Oxford, 1991, pp. 377-382.
[7] Wierzbicki, T., "Crashing Analysis of Metal Honeycombs", *Int. J. Impact Engng.*, Vol. 1, 1983, pp. 157-174.
[8] Reid, S.R., Bell, W.W. and Barr, R., "Structural Plastic Model for One-Dimensional Ring Systems", *Int. J. Impact Engng*., Vol. 1,1983, pp. 185-191.
[9] Shim, V.P.W. and Stronge, W.J., "Lateral Crushing in Tightly Packed Arrays of Thin Walled Metal Tubes", *Int. J. Mech. Sci.*, Vol. 28, 1986, pp. 709-728.
[10] Stronge, W.J. and Shim, V.P.W., "Microdynamics of Crushing in Cellular Solids", *Trans. ASME, J. Engng. Mater. Technol.*, Vol. 110, 1988, pp. 185-190.
[11] Reid, S.R., Peng, C. and Ready, T.Y., "Dynamic Uniaxial Crushing and Penetration of Wood", in *Mechanical Properties of Materials at High Rates of Strain* (ed. J. Harding), Inst. Phys. Conf. Series No. 102, Bristol, 1989, pp. 447-455.
[12] Reid, S.R. and Peng, C., "Dynamic Uniaxial Crushing of Wood", *Int. J. Impact Engng.*, Vol. 19, 1997, pp. 531-570.
[13] Hamada H., "Can Braided Composites Be Used for Crushing Elements in Cars?", 1997, *Proc. ICCM-11*, Vol. I, pp. 218-246.
[14] Chiu C.H. et al., "Energy Absorption of Three-Dimensional Braided Composite Tubes", 1995, *Proc. ICCM-10*, Vol. IV, pp. 187-194.
[15] Chiu C.H. et al., "Crush Behavior of Triaxially Braided Composite Tubes with Different Axial Yarn Content", 1997, *Proc. 4th Asian Textile Conf*. pp. 298-303.
[16] Dreshsler K. et al., "Energy Absorption Behaviour of 3D Woven Sandwich Structures", 1995, Proc. *ICCM-10*, Vol. V, pp. 535-542.
[17] Tao X.M., Yu T.X., Ngan K.M. and Ko F.K., "Energy Absorption of Cellular Textile Composite under Quasi-Static Compression", Hawaii, USA, July, 1997, *Proc. ICCE/4*, pp. 981-982,
[18] Yu T.X., Tao X.M. and Wu K.Q., "Energy Absorption of Cellular Textile Composite under Impact", Hawaii, USA, July, 1997, *Proc. ICCE/4*, pp.1099-1100.
[19] Yu T.X., Tao X.M. and Xue P., "Energy-Absorbing Capacity of Grid-domed Textile Composites", to be published *in Composite Science and Technology*.
[20] Updike, D.P., "On the Large Deformation of a Rigid-plastic Spherical Shell Compressed by a Rigid Plate", *ASME Journal of Engineering for Industry*, No. 94, 1972, pp. 949-955.
[21] Calladine, C.R.,"Analysis of Large Plastic Deformations in Shell Structures", in *Inelastic Behaviour of Plates and Shells* (Proc. of IUTAM Symposium, Rio de Janerro, 1985), L. Bevilacqua, R. Feijoo and R. Valid Eds., pp. 69-101, Springer, 1986.
[22] Calladine, C.R., "Some Problems in Propagating Plasticity", in *Plasticity and Impact Mechanics*, N.K. Gupta Ed, pp. 71-97, Wiley Eastern Ltd., New Delhi, 1993.